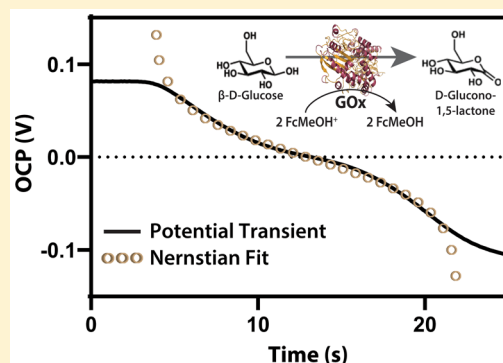


Enzyme Kinetics via Open Circuit Potentiometry

Lettie A. Smith,^{†,§} Matthew W. Glasscott,^{†,§} Kathryn J. Vannoy,[†] and Jeffrey E. Dick^{*,†,§}[†]Department of Chemistry, The University of North Carolina at Chapel Hill, Chapel Hill, North Carolina 27599, United States[§]Lineberger Comprehensive Cancer Center, School of Medicine, The University of North Carolina at Chapel Hill, Chapel Hill, North Carolina 27599, United States

Supporting Information

ABSTRACT: We demonstrate the application of open circuit potentiometry (OCP) to measure enzyme turnover kinetics, k_{turn} . The electrode surface will become poised by the addition of a well-behaved redox pair, such as ferrocenemethanol/ferrocenium methanol ($\text{FcMeOH}/\text{FcMeOH}^+$), which acts as the cosubstrate for the enzymatic process. A measurable change in potential results when an enzyme consumes the one-electron transfer mediator. Glucose oxidase was studied as a test-case, but the method is generalizable across oxidoreductase enzymes that rely on electron transfer mediators. In the presence of glucose and FcMeOH^+ , glucose oxidase delivers electrons to FcMeOH^+ , and the potential changes with respect to the Nernst equation. A theoretical model incorporating enzymatic rate expressions into the Nernst equation was derived to explain the observed potential transients, and experimental data fit theory well. A similar experiment was performed using amperometry on ultramicroelectrodes (UMEs). Here, the same enzymatic rate expression may be incorporated into the equation for steady-state flux to an UME to obtain k_{turn} . While similar kinetic information was obtained from the potentiometric and amperometric responses, potentiometry is independent of electrode size and mass transfer effects. Finally, we show how k_{turn} changes as a function of one-electron mediator. Our results may eventually find applications to biosensors, where electrode fouling plagues long-term sensor performance.



While the applications of electroanalysis to enzymology have been dominated by amperometric and voltammetric techniques,^{1–9} few reports exist regarding potentiometric measurements.¹⁰ Historically, open circuit potential (OCP) has been sparingly used in electroanalysis due to its rather abstract nature and difficulty in achieving specificity. Recently, this technique has been coupled with surface-bound enzymes or nanoparticles for the calibrated detection of various analytes, though a comprehensive understanding of the potential response has not been demonstrated.^{11–15} Perhaps one of the greatest strengths of OCP is that it passes a very small current (i.e., the bias current, i_b , on the order of femtoamperes, 10^{-15} A) while making a measurement. Thus, the OCP differs from amperometric measurements in that OCP permits relatively nondestructive electroanalysis, which may be important in probing small volumes (i.e., within a single cell). Additionally, because of the potential dependence on the Nernst equation, the OCP is independent of electrode size.¹⁶ Therefore, biosensors integrated with OCP sensing techniques may overcome significant issues that amperometric biosensors incur, of which the most problematic is electrode fouling.^{17–20}

Song and colleagues have experimentally shown that OCP can be used to construct an efficient biosensor for glucose detection in vitro and in vivo. By immobilizing glucose oxidase on the surface of the working electrode, they created a selective

biosensor. They demonstrated this selectivity by measuring the OCP in a solution containing glucose and common interferences, such as uric acid, ascorbic acid, and sucrose. This selectivity was expected considering OCP does not involve an applied voltage that would oxidize or reduce interfering molecules at an appreciable rate.¹¹ Song's method was based on the concentration of glucose in solution and depended on the use of a calibration curve, which was comprised of steady state potentials after injecting various concentrations of glucose. A similar method was employed by Charoenkitamorn and colleagues for the detection of human chorionic gonadotropin hormone (hCG).¹²

Collinson and co-workers have made potentiometric measurements of redox mediators and ascorbic acid in buffered solutions and complex matrices. In their initial work with one-electron and two-electron mediators, they demonstrated the ability of OCP to make accurate measurements of mediator concentration in microdroplets. They also found that, when mimicking a biological system by using phosphate buffer and ascorbic acid, they could attain a linear Nernstian plot either at low or high concentrations but not over a large ascorbic acid concentration range.²¹ The same group has extended their

Received: October 31, 2019

Accepted: December 13, 2019

Published: December 13, 2019

study of OCP-based detection of the mediators ferricyanide, ferrocyanide, and ascorbic acid by using blood and human plasma as their sample matrices. In their evaluation of the effectiveness of OCP in more complex matrices, they also examined electrode effects on the OCP response by comparing results when using a nanoporous gold and planar gold electrode.²² The nanoporous gold electrode was shown to experience less biofouling than the planar electrode and was later shown to be capable of long-term sensing of the redox potential of packed red blood cells.^{22,23}

In the 1960s, Malmstadt and Pardue investigated a potentiometric technique as a means to evaluate the kinetics of glucose oxidase using a two-step mechanism involving the oxidation of glucose to gluconolactone and hydrogen peroxide that would result in the production of iodine via a molybdenum catalyst. Their study looked at potentiometric changes due to iodine over time to extract kinetic information on glucose oxidase with its natural cosubstrate, oxygen.¹⁰

Herein, we propose a method and model for determining the kinetics of glucose oxidation by glucose oxidase with several one-electron mediators using both open circuit potentiometry and amperometry. The method involves introducing an enzyme (glucose oxidase) to a solution containing its substrate (D-glucose, which is used interchangeably with glucose throughout this manuscript unless otherwise noted) and a one-electron redox mediator. The potentiometric measurement relies on the potential at the interface of an electrode by an outer-sphere redox pair, which poises the electrode surface. As one of these species is consumed by the enzymatic reaction, the interfacial potential changes according to the Nernst equation. In the amperometric measurement, the current at an ultramicroelectrode (UME) generated by the reduction of the redox mediator decreases as the enzymatic reaction consumes the cosubstrate. Importantly, measurements at the electrode surface act as a reporter for the concentration of oxidant in the bulk solution, which was well-stirred to ensure homogeneity. We demonstrate that k_{turn} may be obtained by both amperometric and potentiometric methods. Interestingly, the result obtained by the amperometric technique is shown to depend on the size of the electrode whereas the potentiometric technique is shown to be independent of electrode size. Potentiometric techniques were used to obtain a calibration curve resembling a Michaelis–Menten plot for the reaction of glucose and glucose oxidase with FcMeOH^+ . Finally, we explored the effect of one-electron transfer mediators, such as ruthenium hexamine and ferricyanide, on the overall enzymatic rate as well as the effect of electrode material.

MATERIALS AND METHODS

Reagents and Materials. All chemicals were of analytical grade unless noted otherwise and were used as received. Glucose oxidase (GOx) and beta-D-Glucose were obtained from MP Biomedicals and were used without further purification. Hydroxymethylferrocene (FcMeOH , 97%) was obtained from Alfa Aesar and bulk electrolyzed to produce ferrocenium methanol for use as a redox mediator. The bulk electrolysis is shown in Figure S1. Other mediators used were hexaammineruthenium(III) chloride (RuHex , 98%) obtained from chemistry and potassium hexacyanoferrate(III) (Fi , $\geq 99.0\%$) obtained from Sigma-Aldrich. Both mediators were used without further purification. Phosphate buffered saline tablets obtained from Fisher Bioreagents were used to make PBS solutions. All mediator and glucose oxidase stock

solutions were made with 1X PBS. Mediator stock solution concentrations were determined using cyclic voltammetry. The cyclic voltammograms of each mediator are shown in Figure S2. All mediators and glucose were stored in a dark box. PBS stock and glucose oxidase stocks were kept in a refrigerator at 4 °C. Glucose oxidase stock was remade every day.

Instrumentation. All open circuit potentiometry experiments were performed on a WaveDriver 200 (Pine Instruments, Durham, NC). Stock mediator concentrations were determined using a CHI model 601E or CHI 920D potentiostat (CH Instruments, Austin, TX) with the cyclic voltammetry technique. All stock solutions were prepared in PBS and sonicated with the exception of the glucose oxidase stock solution. The glucose oxidase stock was vortexed using a vortex-genie (Scientific Industries, New York, Bohemia) in place of sonication. Bulk electrolysis for the production of ferrocenium methanol was carried out using a WaveDriver 200 (Pine Instruments, Durham, NC). Working electrodes used varied in terms of material and radius (5 μm to 1.5 mm). Calibration curve data was collected using a platinum UME ($r = 5 \mu\text{m}$) and a glassy carbon macroelectrode ($r = 1.5 \text{ mm}$). For the different mediator experiments, a glassy carbon macroelectrode ($r = 1.5 \text{ mm}$) was used with respect to ferrocenium methanol (FcMeOH^+) and Fi while a Pt macroelectrode ($r = 1.0 \text{ mm}$) was used with respect to RuHex . Different electrode material experiments were carried out using a macro glassy carbon, gold, and platinum electrode with radii of 1.5, 1.0, and 1.0 mm, respectively. All electrodes used were obtained from CHI. A Ag/AgCl reference electrode with a salt bridge (1 M KCl suspended in agarose) was used for every experiment.

Amperometry Procedure. Solutions were prepared containing ferrocenium methanol (0.5 mM), PBS (1X) at pH 6.8, and glucose oxidase (GOx, 20 nM). Each solution was purged for 15 min using N_2 gas and was sparged using N_2 gas throughout each experiment. A platinum UME, a glassy carbon rod counter, and a Ag/AgCl reference were used. The experiment was carried out at room temperature and each solution was kept in a water bath within a Faraday cage. The current of the solution was measured over time. For each trial, a steady current was measured until approximately 90 s. At 90 s, glucose (150 mM) was injected into the solution through a door in the Faraday cage. After injection, the Faraday cage was immediately closed. The experiment was allowed to run until there was another plateau in current lower than the initial steady current (Figure 3A).

Open Circuit Potentiometry Procedure. Michaelis–Menten Study. To construct a calibration curve of V/s (rate) vs time, solutions containing a 50/50 ratio of ferrocenium methanol to ferrocenemethanol (0.5 mM), PBS (1X) at pH 6.8, and glucose oxidase (20 nM) were prepared. A 50/50 ratio of ferrocenium methanol to ferrocenemethanol was used to ensure the presence of a linear region at low glucose concentrations. Glucose was injected into each solution for various final glucose concentrations (0.5, 6, 8, 10, 20, 30, 40, 50, 75, 100, and 100 mM). The volume of PBS was adjusted depending on the desired final glucose concentration. Each solution was sparged of oxygen using nitrogen gas for 15 min. Once purged, the OCP was measured to record a potential transient plot for each concentration iteration. The experiment was conducted using a glassy carbon macroelectrode ($r = 1.5 \text{ mm}$) and a platinum microelectrode ($r = 5 \mu\text{m}$) (only for glucose concentration of 8, 10, 20, 30, 100, and 100 mM). For every trial, a Ag/AgCl reference with a salt bridge was used.

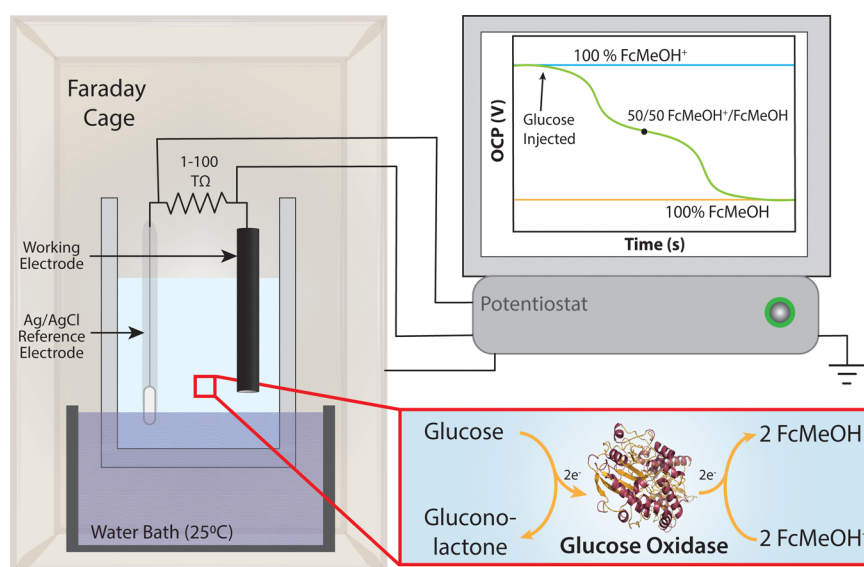


Figure 1. Open circuit potentiometry schematic and theoretical potential transient. A working electrode varying in material (gold, platinum, and glassy carbon) and size ($r = 5 \mu\text{m}$ to 1.5 mm) is placed into a deaerated, temperature-controlled solution of glucose oxidase, redox mediator such as ferrocenium methanol, and phosphate buffered saline. Once a steady potential was reached, the Faraday cage was opened and glucose was injected into solution using a micropipette. This injection led to the oxidation of glucose by GOx, and in turn, the reduction of ferrocenium methanol that corresponds to the potential transient shown on the computer screen.

Each solution was purged using nitrogen gas throughout the experiment. For all runs using the glassy carbon macroelectrode, a stirrer was used for convection. To maintain room temperature, each solution was placed in a water bath. The setup of the experiment is displayed in Figure 1, with the exception of the method of convection because of variation between microelectrode and macroelectrode experiments. Measurements of OCP (V) vs time were taken for approximately 90 s before glucose was introduced into the system. Once 90 s was reached, glucose was injected into solution using a micropipette. The experiment was allowed to run until another plateau in potential was achieved, signifying the total reduction of ferrocenium methanol to ferrocenemethanol. All microelectrode experiments were carried out in a Faraday cage to limit noise. The cage was open for the duration of the glucose injection, and closed otherwise. For each glucose concentration, three trials were conducted.

Different Mediators. Three mediators were used to obtain OCP (V vs Ag/AgCl) vs time plots for the turnover of D-glucose to gluconolactone by glucose oxidase: ferrocenium methanol, hexaammineruthenium(III) chloride, and ferricyanide. Each solution initially contained the mediator of choice (0.5 mM), PBS (1X) at pH 6.8, and glucose oxidase (20 nM) before the injection of 150 mM glucose.

Experiments with the mediators ferrocenium methanol and ferricyanide consisted of an electrochemical cell contained within a Faraday cage. Glucose was injected into the solutions containing these respective mediators by opening the Faraday cage. The Faraday cage was always closed immediately after injection. For the ferrocenium methanol trials, a glassy carbon macroelectrode ($r = 1.5 \text{ mm}$) was used, while a Pt macroelectrode ($r = 1.0 \text{ mm}$) was used for all ferricyanide trials. Solutions containing hexaammineruthenium(III) chloride had to be further isolated using parafilm because of the instability of the mediator's reduced species. A razor blade was used to cut holes into the parafilm to fit the working electrode, reference salt bridge, stirrer, and gas line into the solution.

Glucose was injected by opening the door to the Faraday cage and injecting the glucose through an opening in the parafilm alongside either the working electrode or salt bridge.

Different Electrode Materials. To determine the material independence of the OCP technique, solutions containing ferrocenium methanol (0.5 mM), PBS (1X) at pH 6.8, and glucose oxidase (20 nM) were prepared. OCP was then measured using working electrodes of different materials: glassy carbon, gold, and platinum. All working electrodes used were macroelectrodes ($r = 1.0\text{--}1.5 \text{ mm}$) and three trials were carried out using each electrode material. Glucose (150 mM) was injected into each Solution approx. 90 s after a steady potential was achieved. Concentrations of the species in solution were based off of the final volume (10 mL) of the solution following the injection of glucose. Each trial was conducted at room temperature with the solution contained in a water bath. Convection was maintained during each experiment using a stirrer.

MODEL

We begin with a thought experiment regarding enzymatic turnover rates: if an enzyme and its substrate are mixed homogeneously in a solution, and a cosubstrate is added, the enzymatic reaction progresses. The experiment is outlined in Figure 1. If the cosubstrate is electrochemically active, such as a well-behaved, reversible, one-electron transfer mediator, its concentration can be tracked electrochemically without significantly perturbing the bulk concentration. In this thought experiment, the electrode itself is only acting as a reporter of the bulk concentration of cosubstrate in solution. This experiment works if one assumes homogeneous distribution of electron transfer mediators, which is achieved by mixing the solution either by stirring or sparging with an inert gas. We also imagine electrons are flowing only to the cosubstrate and that competing reactions (i.e., electrons going to oxygen) do not occur in a well-sparged solution.

■ AMPEROMETRY

The steady-state current at an inlaid disk ultramicroelectrode (UME) is given by

$$i = 4nFDrC \quad (1)$$

where i is the current, n is the number of electrons, F is Faraday's constant, D is the diffusion coefficient, r is the radius of the UME, and C is the concentration. In amperometry, we apply 0 V vs Ag/AgCl and reduce FcMeOH^+ to FcMeOH . Because the UME surface is much smaller than the volume of the assay (~ 10 mL), we assume that this reaction does not perturb the bulk concentration of FcMeOH^+ . We are concerned with how the concentration of FcMeOH^+ is changing in the bulk with time due to the enzymatic process, which can be modeled by

$$C_{\text{O}}(t) = C_{\text{O},i} - \frac{msNk_{\text{turn}}t}{N_{\text{A}}V_{\text{cell}}} \quad (2)$$

where $C_{\text{O}}(t)$ is the concentration of O at time, t , $C_{\text{O},i}$ is the initial concentration of O, N is the number of enzymes, m is the stoichiometry of the enzymatic reaction ($m = 2$ for glucose oxidase oxidation, i.e., for every 1 glucose molecule, 2 molecules of O are reduced to 2 molecules of R), s is the number of active sites per enzyme, t is time, N_{A} is Avogadro's number, k_{turn} is the enzymatic turnover rate, and V_{cell} is the volume of the electrochemical cell. This change in concentration will dictate the current–time response in amperometry, following:

$$i(t) = 4nFDr \left(C_{\text{O},i} - \frac{msNk_{\text{turn}}t}{N_{\text{A}}V_{\text{cell}}} \right) \quad (3)$$

where all variables are as previously discussed and $i(t)$ is the change in current with time. Differentiating this equation with respect to time yields a line with the following slope:

$$S = -4nFDr \frac{msNk_{\text{turn}}}{N_{\text{A}}V_{\text{cell}}} \quad (4)$$

which is further simplified to

$$S = -4nFDrmsk_{\text{turn}}C_{\text{enzyme}} \quad (5)$$

where C_{enzyme} is the enzyme concentration. Equations 4 and 5 allow one to calculate enzymatic turnover rates from the amperometric trace. Note the equations also depend on the size of the electrode and diffusion coefficient of the species. Despite sparging the solution during the analysis, we assume the diffusion layer is not perturbed at a small UME surface.

Open Circuit Potentiometry. Consider the oxidation of glucose, which proceeds from glucose oxidase in the presence of one and two-electron transfer mediators and without oxygen, as shown in Figure 2A. Given the electron transfer kinetics of $\text{O} + ne^- \rightarrow \text{R}$ is very fast and reversible, the equilibrium potential of this solution is governed by the Nernst equation that has been corrected for the liquid junction potential:

$$E_{\text{OCP}} = E^0 + \frac{RT}{nF} \ln \left(\frac{C_{\text{O}}^*}{C_{\text{R}}^*} \right) + E_j \quad (6)$$

where E is the open circuit potential, E^0 is the thermodynamic potential, E_j is the liquid junction potential, R is the universal gas constant, T is temperature, n is the number of electrons, F

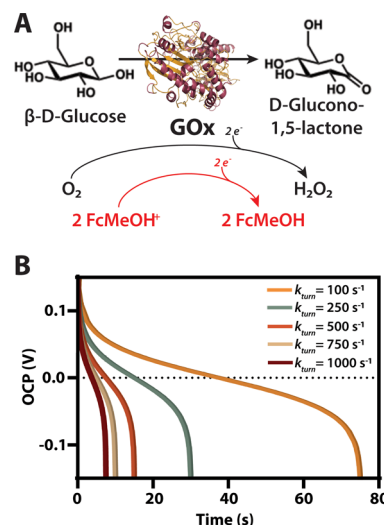


Figure 2. Solution components and theoretical OCP transients. (A) Schematic representation of the oxidation of glucose to gluconolactone by glucose oxidase with varying electron mediators. (B) Theoretical open circuit potential transients for various GOx k_{turn} values.

is the Faraday, C_{O}^* is the bulk concentration of O, C_{R}^* is the bulk concentration of R. When an enzyme is added to the solution, glucose oxidase catalyzes the oxidation of glucose while shuttling electrons to O to produce R. We can ignore the contribution of E^0 and E_j by considering the rate of change, or slope, of the response and assuming that E^0 and E_j are not changing with time. Thus, we can subtract the contributions of these potentials, $E_{\text{OCP}} - E^0 - E_j = \Delta E$, giving the time-dependent Nernst equation

$$\Delta E(t) = \frac{RT}{nF} \ln \left(\frac{\Delta C_{\text{O}}^*(t)}{\Delta C_{\text{R}}^*(t)} \right) \quad (7)$$

where $\Delta C_{\text{O}}^*(t)$ and $\Delta C_{\text{R}}^*(t)$ represent the change in concentration of O and R with time when the enzymatic reaction is active. When the enzyme is added to the solution, O will be consumed and R generated throughout the solution. We assume this reaction is homogeneous throughout the solution. Assuming the rate-limiting step is not the heterogeneous electron transfer (at OCP, the electrode still electronically communicates both anodically and cathodically with solution species), k_{turn} will govern the reaction rate. The concentration of species O and R at time t can be modeled by the following equations involving enzyme kinetics

$$\Delta C_{\text{O}}^*(t) = C_{\text{O},i} - \frac{msNk_{\text{turn}}t}{N_{\text{A}}V_{\text{cell}}} \quad (8)$$

$$\Delta C_{\text{R}}^*(t) = C_{\text{R},i} + \frac{msNk_{\text{turn}}t}{N_{\text{A}}V_{\text{cell}}} \quad (9)$$

where all variables are as previously defined. Using this equation, we arrive at a time-dependent form of the Nernst equation

$$\Delta E(t) = \frac{RT}{nF} \ln \left(\frac{N_{\text{A}}V_{\text{cell}}C_{\text{O},i} - msNk_{\text{turn}}t}{N_{\text{A}}V_{\text{cell}}C_{\text{R},i} + msNk_{\text{turn}}t} \right) \quad (10)$$

This equation is simulated in Figure 2B, which shows several curves as a function of k_{turn} as well as a schematic of the

solution components. From this simulation, it is obvious that there exists a linear region about the transition point where $C_O = C_R$. Differentiation of eq 10 with respect to time allows the determination of the slope, which is given by

$$S = -\frac{4msNk_{\text{turn}}t}{nF N_A V_{\text{cell}}(C_{O,i} + C_{R,i})} \quad (11)$$

Which is further simplified to

$$S = -\frac{4msk_{\text{turn}}C_{\text{enzyme}}t}{nF(C_{O,i} + C_{R,i})} \quad (12)$$

Importantly, note eqs 11 and 12 are independent of electrode size and mass transfer effects.

RESULTS AND DISCUSSION

As discussed in the previous section, one can measure enzyme kinetics with amperometry and voltammetry, and such experiments have been reported.^{5–8} We began our analysis by a simple thought experiment: If a solution of oxidoreductase enzyme meets its substrate, electrons will flow to or from the substrate to an electron acceptor or electron donor. For instance, glucose oxidase generally delivers electrons from glucose to oxygen. However, the enzyme has been shown to deliver electrons to other oxidants (O), such as one-electron mediators like ferrocenium.⁸ UMEs are useful in these experiments due to the rapid diffusion of analyte to the electrode surface (i.e., concentration profiles are unchanging with time). Figure 3A is an example of the current response with time on a 5 μm radius platinum UME placed in 20 nM glucose oxidase and in the presence of 150 mM glucose and

0.5 mM FcMeOH⁺. Upon addition of the enzyme substrate, the redox species resulting in the electrochemical signal is consumed, driving the current to zero. The slope of this decline may be directly related to the k_{turn} of glucose oxidase by differentiating eq 3 with respect to time. The k_{turn} value calculated from the slope was $265 \pm 75 \text{ s}^{-1}$. Importantly, it is obvious from eq 4 that the response depends on the radius of the electrode, r (and, consequently, the diffusion coefficient, D). Therefore, the adsorption of molecules or other entities onto the electrode surface during the measurement is expected to reduce the signal and sensitivity over time.⁹

The same rate law can be introduced into the Nernst equation, which governs the OCP, as shown in the previous section. Importantly to make a fair comparison, we used the same UME in Figure 3A to probe the open circuit potential transient with time (Figure 3B). Figure 3B shows an experimental potential transient (black trace) and the simulated response using eq 10 (gold circles), and the two overlay remarkably well. The k_{turn} value calculated from the slope was $275 \pm 25 \text{ s}^{-1}$, which is virtually the same as the value achieved using amperometry while maintaining independence of electrode size and mass transfer effects. A Student's t test at 95% confidence was performed on the k_{turn} values revealing no statistical difference.

It is important to clarify the defining characteristics of the response, particularly the difference between the simulated results and the experimental results. In the simulation, there is a rapid change at the beginning and end of the assay due to nonexistent solutions to the Nernst equation stemming from the logarithmic function. In experimental reality, different reactions in solution begin to dictate the OCP response. Previous work suggests these new potentials are dictated at the extremes by mixed potentials between oxygen reduction and ferrocenemethanol oxidation (and ferrocenium methanol reduction and water oxidation at the other end).¹⁷ This explanation is grounded in mixed potential theory, for which a detailed derivation and discussion have been given previously.²⁴ Importantly, the derivation in ref 24 also predicts the OCP is independent of electrode size yet renders the same information as eq 3.

The rate of the enzymatic process can be used to calculate the concentration of an analyte of interest due to the dependence of enzymatic activity on substrate concentration. Figure 4A shows potential transients on macroelectrodes as a function of glucose concentration, and Figure 4B shows how the decay rate changes as a function of substrate concentration (a colloquial Michaelis–Menten type of plot). Figure 4C shows potential transients on a platinum ultramicroelectrode as a function of glucose concentration. The large transients seen before 50 s in Figure 4C are from opening and closing the Faraday cage during the assay. Given the similarities in the rate of change, k_{turn} is demonstrated throughout Figure 4 to be independent of electrode size. This difference is difficult to probe amperometrically due to the changing concentration profiles in semi-infinite linear diffusion at macro-electrodes. Figure 4D shows the same Michaelis–Menten type of plot on ultramicroelectrodes. Interestingly, the relative standard deviations on ultramicroelectrodes is less than macroelectrodes. We have also found that consistency in making solutions (stock versus fresh solutions) can be a source of variability. At this time, we cannot explain the observation regarding lower relative standard deviations at ultramicroelectrodes, and this

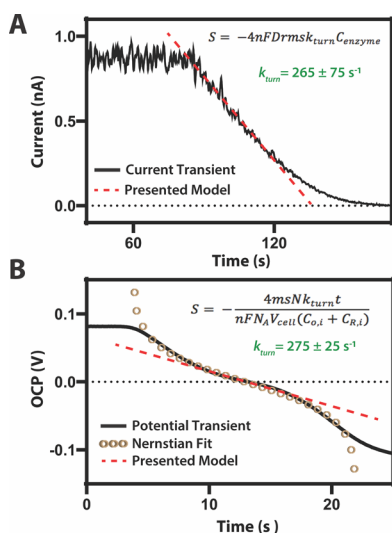


Figure 3. Comparing enzymatic rate-laws for amperometric and OCP techniques on ultramicroelectrodes (radius 5 μm). (A) Amperometric experiment showing a decline in current after the addition of substrate due to the rapid reduction of FcMeOH⁺ by GOx. The dashed red line represents the linear region of the i - t curve, where the slope is directly related to the k_{turn} for glucose oxidase. (B) Potential transient obtained from the reduction of FcMeOH⁺ by GOx after the addition of 150 mM glucose. A Nernstian fit according to eq 3 models the logarithmic behavior of the transient, while the dashed red line indicates the linear region used to extract k_{turn} . A Pt UME, Ag/AgCl reference electrode with a salt bridge, and a glassy carbon rod counter were used for both the amperometric and OCP experiments.

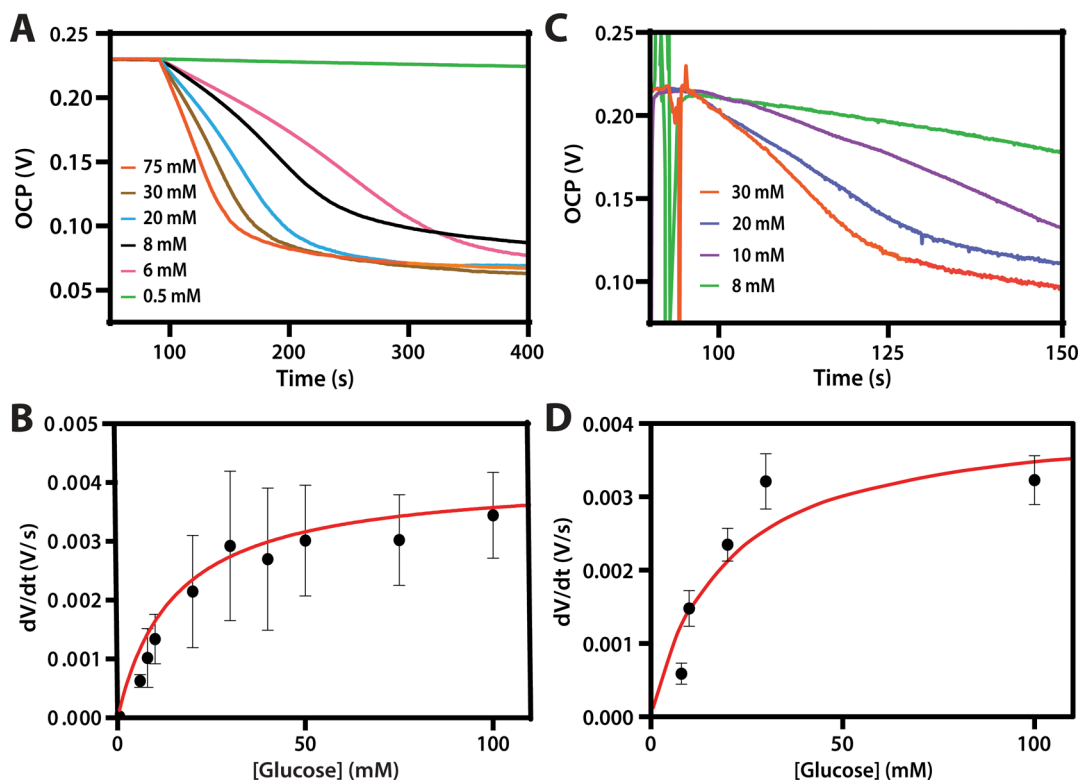


Figure 4. Potential transients and resulting calibration curve. (A) Potential transients on macroelectrodes as a function of glucose concentration. Glucose concentrations ranged from 0.5 to 100 mM. Only a few transients are shown. All transients can be found in Figure S3. A glassy carbon macroelectrode ($r = 1.5$ mm) and Ag/AgCl reference with a salt bridge were used. (B) Calibration curve constructed using slope values from linear regions of potential transients on macroelectrodes for different glucose concentrations. (C) Potential transients on microelectrodes ($r = 5$ μ m) as a function of glucose concentration. The noise prior to 100 s for each curve is a result of opening the Faraday cage to inject glucose into solution. Glucose concentrations ranged from 8 to 100 mM. Only four transients are shown. All transients are displayed in Figure S3. A Ag/AgCl reference with a salt bridge and a Pt UME ($r = 5$ μ m) were used for each experiment. (D) Calibration curve constructed using slope values from linear regions of potential transients on microelectrodes for different glucose concentrations. For each transient, the concentration of glucose oxidase in PBS was 20 nM. Different glucose oxidase stocks were used for the macroelectrode and microelectrode experiments.

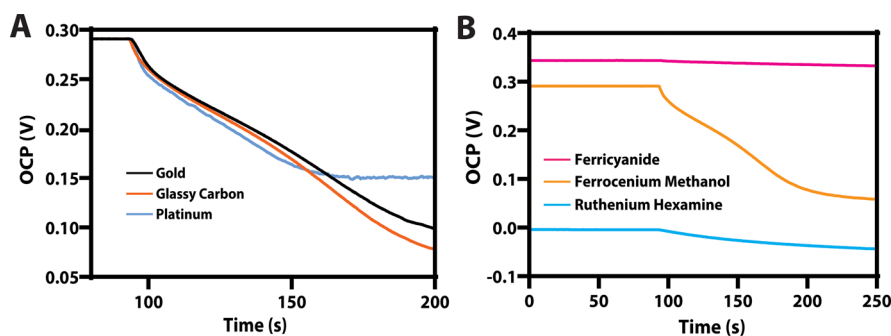


Figure 5. Different electrode material and different mediator effects. (A) Potential transients on macroelectrodes of different material [gold ($r = 1.0$ mm), glassy carbon ($r = 1.5$ mm), and platinum ($r = 1.0$ mm)] with 150 mM glucose. (B) Potential transients on macroelectrodes for different electron mediators (ferricyanide, ferrocenium methanol, and hexaammineruthenium(III) chloride) with 150 mM glucose. For each transient, a Ag/AgCl reference was used with a salt bridge and the concentration of glucose oxidase in PBS was 20 nM.

will be the topic of future investigations. These results indicate that the open circuit response can be used to calculate the substrate concentration if concentrations are within the range of the Michaelis constant, K_M , which is ~ 10 mM and matches reasonably well with reported values measured using O_2 as the cosubstrate.

Because the $FcMeOH/FcMeOH^+$ couple is a fast and reversible heterogeneous process, one would not expect a difference in the value of k_{turn} by varying the electrode material. This is demonstrated in Figure 5A, where values were

measured on gold, glassy carbon, and platinum macroelectrodes. Variations in the potential over long periods of time can be semiquantitatively explained using mixed potential theory. We have also found that the rates depend heavily on the choice of one-electron oxidants. For instance, we have studied ferricyanide, ferrocenium methanol ($FcMeOH^+$), and hexaammineruthenium(III) chloride ($RuHex$) and found variability in slope and, therefore, k_{turn} . The molecular structures for these three species are shown in Figure S5. Figure 5B depicts the potential transients of each of these

mediators. Of the three mediators, FcMeOH⁺ has the steepest slope followed by RuHex and then ferricyanide. From the slope equation in Figure 3B, the k_{turn} corresponding to each mediator was determined to be 198, 64.1, and 8.7 s⁻¹, respectively. At this point in time, it is difficult to understand the variability of k_{turn} values for different one-electron oxidants; however, we have found no correlation with the charge of the redox mediator (cosubstrate) and the potential transient.

While the point of the current study is to verify the proof-of-principle for the measurement of enzyme kinetics via OCP, it is important to consider eventual applicability. For instance, the enzyme turnover rate is highly specific to a certain oxidoreductase enzyme and its substrate. However, if the solution also contained other oxidoreductase enzymes and their corresponding substrates at appreciable concentrations, this turnover would then compete for the O/R couple that is poisoning the electrode surface (either delivering electrons to O or taking electrons from R). Thus, the turnover rate would be convoluted with these competing reactions. A potential way of diagnosing this is by running necessary control experiments to understand the turnover rate of various oxidoreductase enzymes with certain cosubstrates. Another way to mitigate this is to confine both the oxidoreductase enzyme and the cosubstrate to the electrode surface. This can be accomplished by hydrogel technology or the use of direct electron transfer enzymes and will be the topic of future investigations.

We would also like to address the electrode impedance. The size of the electrode would come into play if the electrode were small enough such that its impedance would be greater than the input impedance of the voltage amplifier (~1 TΩ). We can easily calculate the electrode impedance as a function of electrode radius by $Z_{\text{electrode}} = (4\kappa a)^{-1}$,²⁵ where κ is the solution conductivity (~1 S m⁻¹ for a 100 mM electrolyte solution) and a is the radius of the electrode. Thus, a 1 nm radius electrode would have a total resistance of ~0.2 GΩ, which is much less than the input impedance for common voltage amplifiers (~1 TΩ). This indicates that for all practical purposes, the electrode surface cannot foul enough to disrupt an ongoing measurement.

CONCLUSIONS

We have demonstrated that the open circuit potential is a useful tool in studying enzyme kinetics. Furthermore, the technique is shown to give similar information as amperometry and voltammetry with the added benefit of being independent of electrode size and mass transfer effects. The only drawback to the presented method arises from the presence of oxygen within the system despite purging with nitrogen gas. The presence of oxygen results in a slightly skewed k_{turn} value for glucose oxidase because oxygen competes with the one-electron mediator for electrons (Figure S6). Regardless of the influence of oxygen, the experimental results match the discussed model, showcasing the validity of the presented method. The fact that open circuit potential can be used to study enzyme kinetics indicates that the technique can be used to specifically detect analytes of interest without regard of electrode size. These results may find applications in the fields of wearable and implantable sensors, where sensor longevity has been a critical issue.

ASSOCIATED CONTENT

Supporting Information

The Supporting Information is available free of charge at <https://pubs.acs.org/doi/10.1021/acs.analchem.9b04972>.

Bulk electrolysis curves, cyclic voltammograms of one-electron mediators, potential transient examples, a linear region example, one-electron mediator structures, and transient curves under ambient (including O₂) conditions (PDF)

AUTHOR INFORMATION

Corresponding Author

*E-mail: jedick@email.unc.edu. Telephone: +1-919-966-5229.

ORCID

Matthew W. Glasscott: 0000-0001-5743-7738

Jeffrey E. Dick: 0000-0002-4538-9705

Author Contributions

[§]L.A.S. and M.W.G. contributed equally to this work.

Notes

The authors declare no competing financial interest.

ACKNOWLEDGMENTS

We gratefully acknowledge the University of North Carolina at Chapel Hill for start-up funds, which supported this work. J.E.D. thanks Collin McKinney, R. Mark Wightman, and Koji Sode for helpful discussions.

REFERENCES

- (1) Shumyantseva, V. V.; Kuzikov, A. V.; Masamrekh, A. R.; Bulko, T. V.; Archakov, A. I. *Biosens. Bioelectron.* **2018**, *121*, 192–204.
- (2) Limoges, B.; Marchal, D.; Mavré, F.; Savéant, J. J. *Am. Chem. Soc.* **2006**, *128* (6), 2084–2092.
- (3) Hoebe, F. J.; Meijer, F. S.; Dekker, C.; Albracht, S. P. J.; Herring, H. A.; Lemay, S. G. *ACS Nano* **2008**, *2* (12), 2497–2504.
- (4) Kätelhön, E.; Sepunaru, L.; Karyakin, A. A.; Compton, R. G. *ACS Catal.* **2016**, *6* (12), 8313–8320.
- (5) Cass, A. E. G.; et al. *Anal. Chem.* **1984**, *56*, 667–671.
- (6) Flexer, V.; Ielmini, M. V.; Calvo, E. J.; Bartlett, P. N. *Bioelectrochemistry* **2008**, *74*, 201–209.
- (7) Léger, C.; et al. *Biochemistry* **2003**, *42*, 8653–8662.
- (8) Yokoyama, K.; Kayanuma, Y. *Anal. Chem.* **1998**, *70*, 3368–3376.
- (9) Rocchitta, G.; et al. *Sensors* **2016**, *16*, 780.
- (10) Malmstadt, H. V.; Pardue, H. L. *Anal. Chem.* **1961**, *33* (8), 1040–1047.
- (11) Song, Y.; Su, D.; Shen, Y.; Liu, H.; Wang, L. *Anal. Bioanal. Chem.* **2017**, *409*, 161–168.
- (12) Charoenkitamorn, K.; Tue, P. T.; Kawai, K.; Chailapakul, O.; Takamura, Y. *Sensors* **2018**, *18*, 444.
- (13) Su, D.; Feng, B.; Xu, P.; Zeng, Q.; Shan, B.; Song, Y. *Anal. Methods* **2018**, *10*, 4320–4328.
- (14) Wong, L. C. C.; Jolly, P.; Estrela, P. *BioNanoScience* **2018**, *8*, 701–706.
- (15) Lee, I.; Loew, N.; Tsugawa, W.; Ikebukuro, K.; Sode, K. *Biosens. Bioelectron.* **2019**, *124*, 216–223.
- (16) Park, J. H.; Hongjun, Z.; Percival, S. J.; Zhang, B.; Fan, F. F.; Bard, A. J. *Anal. Chem.* **2013**, *85*, 964–970.
- (17) McCreery, R. L. *Chem. Rev.* **2008**, *108*, 2646–2687.
- (18) MGilmartin, M. A. T.; Hart, J. P. *Analyst* **1995**, *120*, 1029–1045.
- (19) Zhang, G.; et al. *J. Am. Chem. Soc.* **2014**, *136*, 11444–11451.
- (20) Sharma, S.; Singh, N.; Tomar, V.; Chandra, R. *Biosens. Bioelectron.* **2018**, *107*, 76–93.

- (21) Freeman, C. J.; Farghaly, A. A.; Choudhary, H.; Chavis, A. E.; Brady, K. T.; Reiner, J. E.; Collinson, M. M. *Anal. Chem.* **2016**, *88* (7), 3768–3774.
- (22) Farghaly, A. A.; Lam, M.; Freeman, J. C.; Uppalapati, B.; Collinson, M. M. *J. Electrochem. Soc.* **2016**, *163* (4), H3083–H3087.
- (23) Khan, R. K.; Gadiraju, S. P.; Kumar, M.; Hatmaker, G. A.; Fisher, B. J.; Natarajan, R.; Reiner, J. E.; Collinson, M. M. *ACS Sens.* **2018**, *3* (8), 1601–1608.
- (24) Percival, S. J.; Bard, A. J. *Anal. Chem.* **2017**, *89*, 9843–9849.
- (25) Newman, J. J. *Electrochem. Soc.* **1966**, *113*, 501–502.